Systemic infusions of anti-interleukin-1β neutralizing antibodies reduce short-term brain injury after cerebral ischemia in the ovine fetus

Xiaodi Chen[1], **Virginia Hovanesian**[2], **Syed Naqvi**[1], **Yow-Pin Lim**[3], **Richard Tucker**[1], **John E. Donahue**[4], **Edward G. Stopa**[4], and **Barbara S. Stonestreet**[1]

[1]Department of Pediatrics, the Alpert Medical School of Brown University, Women & Infants Hospital of Rhode Island, Providence, RI

[2]Core Research Laboratories, the Alpert Medical School of Brown University, Rhode Island Hospital, Providence, RI

[3]ProThera Biologics, Inc, Providence, RI

[4]Department of Pathology and Neurosurgery, the Alpert Medical School of Brown University, Rhode Island Hospital, Providence, RI

Abstract

Perinatal hypoxic-ischemic reperfusion (I/R)-related brain injury is a leading cause of neurologic morbidity and life-long disability in children. Infants exposed to I/R brain injury develop long-term cognitive and behavioral deficits, placing a large burden on parents and society. Therapeutic strategies are currently not available for infants with I/R brain damage, except for hypothermia, which can only be used in full term infants with hypoxic-ischemic encephalopathy (HIE). Moreover, hypothermia is only partially protective. Pro-inflammatory cytokines are key contributors to the pathogenesis of perinatal I/R brain injury. Interleukin-1β (IL-1β) is a critical pro-inflammatory cytokine, which has been shown to predict the severity of HIE in infants. We have previously shown that systemic infusions of mouse anti-ovine IL-1β monoclonal antibody (mAb) into fetal sheep resulted in anti-IL-1β mAb penetration into brain, reduced I/R-related increases in IL-1β expression and blood-brain barrier (BBB) dysfunction in fetal brain. The purpose of the current study was to examine the effects of systemic infusions of anti-IL-1β mAb on short-term I/R-related parenchymal brain injury in the fetus by examining: 1) histopathological changes, 2) apoptosis and caspase-3 activity, 3) neuronal degeneration 4) reactive gliosis and 5) myelin basic protein (MBP) immunohistochemical staining. The study groups included non-ischemic controls, placebo-treated ischemic, and anti-IL-1β mAb treated ischemic fetal sheep at

Correspondence Author: Barbara S. Stonestreet, M.D., The Alpert Medical School of Brown University, Department of Pediatrics, Women & Infants Hospital of Rhode Island, 101 Dudley Street, Providence, RI 02905-2499, Phone: (401) 274-1122 ext. 47429, Fax: (401) 453-7571, bstonestreet@wihri.org.

Conflict of interest statement

All authors declare that there are no conflicts of interest.

127 days of gestation. The systemic intravenous infusions of anti-IL-1β mAb were administered at fifteen minutes and four hours after *in utero* brain ischemia. The duration of each infusion was two hours. Parenchymal brain injury was evaluated by determining pathological injury scores, ApopTag® positive cells/mm², caspase-3 activity, Fluoro-Jade B positive cells/mm², glial fibrillary acidic protein (GFAP) and MBP staining in the brains of fetal sheep 24 h after 30 min of ischemia. Treatment with anti-IL-1β mAb reduced (*P<0.05*) the global pathological injury scores, number of apoptotic positive cells/mm², and caspase-3 activity after ischemia in fetal sheep. The regional pathological scores and Fluoro-Jade B positive cells/mm² did not differ between the placebo- and anti-IL-1β mAb treated ischemic fetal sheep. The percent of the cortical area stained for GFAP was lower (*P<0.05*) in the placebo ischemic treated than in the non-ischemic group, but did not differ between the placebo- and anti-IL-1β mAb treated ischemic groups. MBP immunohistochemical expression did not differ among the groups. In conclusion, infusions of anti-IL-1β mAb attenuate short-term I/R-related histopathological tissue injury, apoptosis, and reduce I/R-related increases in caspase-3 activity in ovine fetal brain. Therefore, systemic infusions of anti-IL-1β mAb attenuate short-term I/R-related parenchymal brain injury after in the fetus.

Keywords

apoptosis; blood-brain barrier; caspase-3; cytokines; interleukin-1β; ischemia-reperfusion; monoclonal antibody; ovine fetus

1. Introduction

Perinatal hypoxic-ischemic reperfusion (I/R) results in cerebral palsy (CP), seizures (Vannucci, 2000), and neurodevelopmental delay, and is one of the most severe disabilities in childhood (Newacheck and Taylor, 1992; Pharoah, 1985; Stanley, 1994). The early response of developing brain to I/R is characterized by apoptotic/necrotic cell death resulting from excitatory neurotoxicity, free oxygen radical production, oxidative stress, and mitochondrial dysfunction (Ferriero, 2004; Ten and Starkov, 2012). Selective targeting of these early indicators of injury has not yielded effective neuroprotective strategies most likely because this injury is not reversible (Leonardo and Pennypacker, 2009). Neuroinflammation with the release of pro-inflammatory cytokines contributes to the delayed responses to I/R in the developing brain (Bhalala et al., 2014). Accumulating evidence suggests that inhibiting the upregulation of pro-inflammatory cytokines could be an important neuroprotective strategy (Carty et al., 2008; Chew et al., 2006; Tang et al., 2010).

Increases in systemic inflammatory states including sepsis, necrotizing enterocolitis, and prolonged mechanical ventilation cause or exacerbate brain injury in premature and full term neonates (Bose et al., 2013; Stoll et al., 2004; Walsh et al., 2005). Pro-inflammatory cytokines are increased in the circulation of neonates after I/R brain injury, and correlate with the severity of injury and abnormal neurodevelopmental outcomes (Back, 2006; Bartha et al., 2004; Liu and Feng, 2010).

Interleukin-1β (IL-1β) is among the best-characterized pro-inflammatory cytokines (McAdams and Juul, 2012; Silverstein et al., 1997). Human newborns with hypoxic-ischemic encephalopathy (HIE) have high levels of IL-1β in peripheral blood and the IL-1β

levels show positive correlations with the severity of HIE (Liu and Feng, 2010; Oygur et al., 1998). In addition, we have shown that systemic IL-1β can penetrate the I/R-injured BBB potentially contributing further to parenchymal brain damage (Sadowska et al., 2015).

The most frequent strategy used to inhibit the effects of IL-1β is the IL-1 receptor antagonist (IL-1ra). This receptor agonist competitively inhibits IL-1β activity and protects adult and neonatal brains from HI injury (Lan et al., 2015; Martin et al., 1994; Relton et al., 1996; Savard et al., 2015; Savard et al., 2013). However, we have recently produced and purified a specific and sensitive mouse anti-ovine interleukin-1β mAb for use in fetal sheep (Chen et al., 2013; Rothel et al., 1997). This mAb effectively neutralizes the effects of ovine IL-1β protein (Chen et al., 2013; Rothel et al., 1997). We have previously infused this mAb systemically into the ovine fetus with I/R brain injury, and showed that the anti-IL-1β mAb 1) resulted in mAb accumulation within the fetal brain parenchyma; 2) reduced I/R-related increases in systemic IL-1β brain penetration and endogenous IL-1β brain expression; and 3) inhibited I/R-related BBB leakage (Chen et al., 2015; Patra et al., 2017). The objective of the current study was to determine whether systemic infusions of anti-IL-1β mAb exert neuroprotective effects on short-term I/R-related parenchymal brain injury in the fetus by examining: 1) histopathological changes, 2) apoptosis by *in situ DNA fragmentation* and caspase-3 activity, 3) neuronal degeneration, 4) reactive gliosis and 5) myelin basic protein expression.

2. Methods

The present study was conducted after approval by the Institutional Animal Care and Use Committees of the Alpert Medical School of Brown University and Women & Infants Hospital of Rhode Island in accordance with the National Institutes of Health Guidelines for the use of experimental animals.

2.1. Anti-IL-1β mAb production and purification

The anti-IL-1β mAb was generated with mouse hybridoma cells using previously described methods (Chen et al., 2013; Rothel et al., 1997; Seow et al., 1994; Wood et al., 1990). Details regarding the methods for purification of anti-IL-1β mAb have also been reported (Chen et al., 2015; Chen et al., 2013). The mouse hybridoma cells were generously supplied by Commonwealth Scientific and Industrial Research Organization (CSIRO, Livestock Industries, Victoria, Australia).

2.2. Animal preparation, study groups, and experimental design

Brain tissue samples for the present study were obtained from animals in our previous published studies (Chen et al., 2015; Chen et al., 2012; Patra et al., 2017; Sadowska et al., 2015). The surgical preparation techniques and physiological measures have been previously reported in detail (Chen et al., 2012; Petersson et al., 2002; Stonestreet et al., 1999). Briefly, the surgical procedures including the laparotomy and hysterotomy on the ewe, the insertion of indwelling catheters, placement of the occluders and electrocorticogram (ECoG) leads, and ligation of the lingual arteries and vertebral-occipital anastomoses to restrict blood flow

from non-cerebral and vertebral sources in the fetus were performed under 1–2% isoflurane anesthesia on mixed breed pregnant ewes at 120 to 122 days-of-gestation (term=145 days).

The design of our study is schematically shown in Fig. 1A. The ewes were allowed to recover for 6–7 days after surgery, and then randomly assigned to three groups: 1) Non-instrumented non-ischemic sham control (Control, n=5–16), 2) instrumented animals with 24-h of reperfusion after 30 min of carotid occlusion, hereafter designated as ischemic (Isch), treated with placebo (Isch-PL, n=10–14), or 3) treated with anti-IL-1β mAb (Isch-mAb, n=10–12). After the baseline determinations, ischemia was induced by inflating the carotid occluders for 30 min. At the end of ischemia, the occluders were deflated and reperfusion continued for 24 h. Therefore, we have examined short-term recovery from ischemia in the current study. The duration of reperfusion was selected based upon the optimal time of reperfusion for our previous BBB permeability studies (Chen et al., 2012). Intravenous placebo (0.154 M NaCl) or anti-IL-1β mAb [5.1±0.6 mg/kg, mean ± standard deviation (SD)] infusions were given at 15 min and 4 h after brain ischemia (Chen et al., 2015). The initial phase of the anti-IL-1β mAb infusion was given over 2-hours beginning 15 minutes after ischemia. An additional anti-IL-1β mAb infusion was also given over 2 h beginning 4 h after ischemia. The infusion paradigm was designed to achieve early-sustained increases in systemic mAb levels in order to expose the cerebral microvasculature to mAb for a prolonged time after ischemia and before onset of BBB permeability studies (Chen et al., 2015). The infusion was planned so that the fetal sheep would receive a slow exposure to the mAb because we were not able to predict the response of the fetal sheep to systemic IL-1β inhibition. This infusion regimen did produce steady-state levels of mAbs during the studies (Chen et al., 2015). We gave the two infusions because we did not know if the presence of the placenta in the fetus would affect the mAbs levels.

The fetal sheep were approximately 123–127 days and 85% of gestation at the end of the studies. The fetal sheep brain at 85% percent of gestation is generally thought to be similar to the brain of the near term human infant (Gunn et al., 1997). The fetal brain was rapidly removed and weighed at the end of the studies. Fig. 1B schematically illustrates the sections of the brain used for analysis. One-half of the fetal brain was dissected to measure regional BBB permeability for our previous studies as shown by the shaded light gray area (Chen et al., 2015; Chen et al., 2012; Patra et al., 2017; Sadowska et al., 2015). The residual brain tissue was saved for analysis and used in the current study. The dark gray shaded area shows the section of the brain used for histopathological analysis. The black circle shows the area of frozen cerebral cortical tissue used for caspase-3 activity, and the black square shows the area used for ApopTag, Fluoro-Jade B (FJB), glial fibrillary acidic protein (GFAP) and myelin basic protein (MBP) staining.

The coronal brain sections (Fig. 1B) that were obtained at the level of the hypothalamus (mammillary bodies) were immersion-fixed in 4% paraformaldehyde (PFA) as previously described (Elitt et al., 2003; Petersson et al., 2002; Petersson et al., 2004). These hemi-brain sections were used for the histopathological analysis. The residual brain tissue was immediately frozen and kept at −80°C until analysis.

2.3. Pathological analysis

The paraffin-embedded brain sections (10-μm) were stained with Luxol fast blue/ hematoxylin eosin (LFB/H&E). The well-established scoring system of Williams *et al.* (Williams et al., 1992) was modified to include scores for gray and white matter, parasagittal gray and white matter (Petersson et al., 2002). Two neuropathologists, who were not aware of study groups, scored the brain sections based upon the percent of neuronal and white matter damage. The pathologists scored the most severely injured area of each section using a grading system (0–5): in which 0 = 0% focal ischemic injury, 1 = 1–10%, 2 = 11–50%, 3 = 51–90%, 4 = 91–99% and 5 = 100% (Elitt et al., 2003; Petersson et al., 2002; Petersson et al., 2004; Williams et al., 1992). In addition, a global injury score for damage to the entire hemi-brain section was added to the current analysis. The overall global injury score represented the total amount of the damaged area in the hemi-brain section. The global score was performed using the following scale: 0 = 0%, 1 = 1–20%, 2 = 21–40%, 3 = 41–60%, 4 = 61–80% and 5 = 81–100%. Nuclear pyknosis, cytoplasmic reddening and condensation, and hyperchromatism were indicative of neuronal injury, whereas myelin degradation and reactive gliosis were indicative of white matter damage (Brown and Brierley, 1972; Elitt et al., 2003; Williams et al., 1992).

2.4. Immunohistochemical staining

Frozen fetal cerebral cortical tissues were sectioned at 6 μm (Leica Cryocut 1800). Sections were mounted on Superfrost Plus slides and stored at –80°C until required for analysis. One slide was stained with LFB/H&E to determine the entire surface area of the cerebral cortical tissue for each fetal sheep brain.

Brain cryosections were air-dried for 30 min and fixed in 4% PFA for 10 min at room temperature. Sections were incubated in phosphate-buffered saline (PBS) containing 0.1% Triton X-100 (Sigma-Aldrich, St. Louis, MO, USA) for 10 min after having been washed 3 times with PBS for 10 min each. The sections were incubated with blocking buffer (1% BSA, 5% normal goat serum and 0.1% Triton X-100 in PBS) combined with 0.3 M glycine for 2 h to block non-specific binding of the antibodies. The primary and secondary antibodies (Abs) were diluted in the blocking buffer as follows: 1) primary Abs: mouse anti-Fox3/neuronal nuclei (NeuN) monoclonal antibody (mAb, 1:500, Abcam, Cambridge, MA, USA), chicken anti-GFAP polyclonal antibody (pAb, 1:1000, Abcam), mouse anti-MBP mAb (1:200, Abcam); 2) secondary Abs: Alexa Fluor® 555 goat anti-mouse IgG (1:500, Thermo Fisher Scientific, Carlsbad, CA, USA), Alexa Fluor® 555 goat anti-chicken IgG (1:1000, Thermo Fisher Scientific). Sections were incubated with primary Abs overnight at 4°C, and then washed three times with PBS for 5 min each. After incubation with secondary Abs for 1 h at room temperature in the dark, the sections were washed in PBS and mounted in Vectashield antifade mounting media (H-1200, Vector Laboratories, Burlingame, CA, USA) containing 1.5 μg/ml 4′,6-diamidino-2-phenylindole (DAPI).

2.5. Double-fluorescent labeling for in situ DNA fragmentation and NeuN, and caspase-3 cleavage assay

Brain cryosections obtained from the cerebral cortex as described above (2.4) were first stained with mouse anti-NeuN mAb (1:200, Abcam) as above, and then labeled for DNA

fragmentation using the ApopTag® Plus In Situ Apoptosis Fluorescein Detection Kit (S711, EMD Millipore, Billerica, MA, USA). This Kit distinguishes apoptosis from necrosis by specifically detecting DNA cleavage and chromatin condensation associated with apoptotic cells *in situ* with the indirect TUNEL method by using an anti-digoxigenin antibody conjugated to a fluorescein reporter molecule.

The sections were incubated with equilibration buffer for 1 min and consecutively with TdT enzyme (30%, v/v) in a humidified chamber at 37°C for 1 h after having been stained for NeuN. The TdT enzyme reaction was terminated by incubating with stop/wash buffer (3%, v/v) for 10 min at room temperature. The sections were incubated with pre-warmed anti-digoxigenin conjugate (47%, v/v) in a humidified chamber for 30 min at room temperature in a dark room after having been washed in PBS three times for 1 min each. The sections were then rinsed with PBS and mounted on slides with Vectashield antifade mounting media (H-1200, Vector Laboratories) containing 1.5 μg/ml DAPI. The ApopTag assay was validated along with a set of negative and positive controls provided by the manufacturer (EMD Millipore). Furthermore, our previous study showed that similar methodology demonstrated adequate staining of sheep cerebral cortical cells with the typical morphologic characteristics of apoptosis, and minimal background staining of the negative control sheep sections (Malaeb et al., 2009).

A microscopist, who was not aware of the study group designations, analyzed equivalent areas of cerebral cortex from each fetal sheep within the three study groups. Cell counts for NeuN, ApopTag and FJB-positive cells in the cerebral cortex were visually counted using a Nikon E800 microscope (Nikon Inc, Melviille, NY) with a 40× Plan Apo objective. The relative cellular density of the cerebral cortical sections was determined to be homogeneous and similar among the three groups of fetal sheep (Malaeb et al., 2009). Therefore, the entire surface area of each cerebral cortical section was measured on the LFB/H&E stained section and was used to determine the density of the immunoreactive positive cells per square surface area. The LFB/H&E sections were scanned with a Nikon CoolScan 5000 to determine the total surface area (Nikon, Inc, Melville, NY). The area measurements were performed with Image J (NIH, Springfield VA, USA). The LFB/H&E images were converted to a grayscale, thresholded and calibrated so that the final results are expressed as number of cells per millimeter squared (mm^2).

The immunoreactivity of GFAP and MBP were determined by acquiring four randomly selected 8-bit grayscale images (field area) with a Zeiss ImagerM2 (Carl Zeiss Microscopy, Munich, Germany) and an AxioCam camera (Carl Zeiss Microscopy, Munich, Germany) using a 10× Neofluor objective. The image processing and analysis was performed using Image J (NIH). Positive stained areas for GFAP and MBP were defined through intensity thresholding and the resulting binary images were measured for the positively stained areas. The ratio of immunoreactive positive MBP or GFAP areas to the total field area was designated as the percent of the total area, and the ratio of immunoreactive positive areas of MBP to GFAP were calculated.

Caspase-3 enzymatic activity was determined by a fluorometric assay according to Chung et al. (Chung et al., 2000) with some additional modifications on a homogenate of the frozen

cerebral cortical tissue. Approximately 0.1 g of the fresh frozen tissue adjacent to the area used for microscopic analyses was homogenized in 1 mL of buffer [25 mM HEPES at pH 7.4, 5 mM MgCl$_2$, 1 mM EGTA, 1 μg/mL aprotinin and leupeptin (Sigma-Adrich), 0.04 mg/ml Pefabloc SC (Roche, Mannheim, Germany), 2% PSF protector solution (Roche)]. It was incubated on ice for 30 min and then centrifuged at 100 g for 5 min followed by an additional 30 min centrifugation at 16,000 g for 30 min at 4°C. The supernatant was collected and its protein concentration determined by a bicinchoninic acid protein assay (BCA; Pierce, Rockford, IL, USA). One hundred μg of lysate along with 20 μl homogenization buffer was loaded into a black 96-well plate and incubated with 100 μl of AFC buffer [(100 mM HEPES at pH 7.4), 2% sucrose, 0.2% CHAPS (Sigma-Adrich),10 mM DTT, 50 μM Asp-Glu-Val-Asp-7-Amino-4-trifluoromethylcoumarin (DEVD-AFC, BioVision, Milpitas, CA, USA). AFC (BioVision)] was used to obtain a standard curve along with the cytosolic Jurkat extract produced by the addition of 2 μM camptothecin (BioVision) as a positive control (Malaeb et al., 2009). Fluorescence was measured at an excitation wavelength of 400 nm at 0, 20, 40, 60, 80, 100, and 120 min at 37°C and emission measured at 505 nm with the use of a multi-detection microplate reader (Spectromax M5, Molecular Devices, Sunnyvale, CA, USA). Enzyme activity was calculated as picomoles per milligram protein per minute (Manabat et al., 2003).

2.6. Fluro-Jade B (FJB) fluorescent staining

Fluro-Jade B (FJB) is an anionic fluorescent stain used to identify dying/degenerating neurons (Rosen et al., 2006; Schmued et al., 1997; Schmued and Hopkins, 2000). The cryosections were double-stained with an anti-NeuN mAb in order to avoid counting non-specific FJB staining in cell fragments and vascular elements. NeuN is a pan-neuronal marker in vertebrates. Double-stained NeuN/FJB positive cells were used for counting. The current protocol was performed as described by Rosen et al. with additional modifications (Rosen et al., 2006). Cerebral cortical cryosections were first stained with mouse anti-NeuN mAb (1:200, Abcam) as described above. The sections were washed three times (10 min each) in PBS, followed by a 5 min rinse in distilled water (dH$_2$O) after incubation with secondary Ab. The sections were then agitated on a shaker in 0.06% KMnO$_4$ for 10 min, and rinsed with dH$_2$O two times for 2 min each. The sections were incubated in a 0.0004% of FJB (Sigma-Adrich) for 30 min and rinsed three times for 2 min each in dH$_2$O. The sections were counterstained with DAPI (300 nM, Thermo Fisher Scientific) for 30 min and rinsed twice for 2 min each in dH$_2$O, then cleaned in xylene, mounted and cover-slipped with Vectashield antifade mounting media (H-1000, Vector Laboratories).

2.7. Statistical analyses

Ordinal regression using SAS GLIMMIX generalized mixed modeling was used to analyze the pathological injury scores. Least squares means were used for group differences and P values were obtained by Tukey-Kramer test after adjustment for multiple comparisons. A statistical package (Statistica, StatSoft, Tulsa, OK, USA) was used to analyze the cell counts that included ApopTag/NeuN and FJB/NeuN positive cells, to determine the percent of the GFAP and MBP positive areas, caspase-3 activity, and for the correlation analyses. A normality test (Shapiro-Wilk's W test) was first used to test the distributions of data obtained within the experimental groups. The normally distributed data included the ApopTag/NeuN

positively stained cell counts and caspase-3 enzymatic activity. These determinations were analyzed by one-way analysis of variance (ANOVA) to detect differences among the three study groups. If a significant difference was detected by ANOVA the Fisher's least significant difference (LSD) method for multiple comparisons was used as a post hoc test. Data that was not normally distributed included the FJB/NeuN positively stained cell counts and the percent of the GFAP and MBP positive areas. These determinations were analyzed with the Kruskal-Wallis ANOVA and median test to determine differences among the multiple independent groups. If a significant difference was found, the analysis of multiple comparisons of mean ranks for the groups was used to identify specific differences between groups. Correlational analysis was used to compare the relationship of the global pathological scores and total ApopTag positive cells/mm^2, and ApopTag/Non-neuronal positive cells/mm^2. In our analyses *P<0.05* was considered statistically significant.

3. Results

The gestational ages, brain, and fetal body weights did not differ among Control, Isch-PL, and Isch-mAb groups. The physiological variables monitored during the studies were within the physiological range for fetal sheep at this gestational age. The arterial pH, pO_2 and pCO_2, heart rate, mean arterial blood pressure, lactate, and hematocrit levels were all within the normal range during the studies and did not change within or among the study groups (Chen et al., 2015; Patra et al., 2017; Sadowska et al., 2015). The amplitude of ECoG signal was attenuated and became equally isoelectric in both the PL- and mAb-treated I/R groups, and the carotid arterial blood flow indicated near zero flow during the 30-min ischemic exposure suggesting that the ischemia was adequate (Chen et al., 2015; Chen et al., 2012; Patra et al., 2017; Sadowska et al., 2015). The systemic infusions of anti-IL-1β-mAb resulted in relatively stable elevated plasma mAb levels from 4 until 25 h at the end of study, which confirmed sustained systemic exposure to mAb during the studies (Chen et al., 2015; Patra et al., 2017).

3.1. Systemic infusions of anti-IL-1β-mAb attenuate I/R-related short-term parenchymal brain injury

Fig 2. shows a coronal section of the hemi-brain at the level of the hypothalamus (mammillary bodies) from a sham Control (A), placebo treated fetus exposed to 30 min of ischemia and 24 h of reperfusion (B, Isch-PL), and anti-IL-1β mAb treated ischemic (C, Isch-mAb) fetal sheep brain stained with LFB/H&E. The section from the Control (A) exhibits homogenous blue stained myelin and healthy appearing cerebral cortex. This represents a score of zero. In contrast, the section from the Isch-PL group shows a shrunken cerebral cortical section with decreased blue stained myelin indicating white matter loss and marked thinning of the cerebral cortex suggesting neuronal loss. This represents a score of 4. The section from the Isch-mAb group shows more of the blue stained myelin suggesting relative preservation of the white matter. The comparatively healthy appearance of the cerebral cortex also suggests cortical preservation. This represents a score of one. These findings can be interpretive to suggest that systemic intravenous infusions of anti-IL-1β mAb have beneficial neuroprotective effects on short-term brain injury in the brain of the ovine fetus.

Fig. 3A contains representative sections of LFB/H&E stained brain from the Control (n=5), Isch-PL (n=11), and Isch-mAb (n=12) groups. The histological panels shown are representative of the mean scores shown in 3B. The entire cerebral cortical section in the Control animals showed homogeneous healthy-appearing neurons with a well-defined nucleus and Nissl substance distributed throughout the cytoplasm (A, arrow, left panel) and white matter with homogenously blue-stained myelin. The insets show the whole hemi-brain sections in each group that were examined by the neuropathologists. Sections from the fetuses exposed to I/R exhibited damage to the cerebral cortex (A, Isch-PL, middle panel). These areas showed pallor on LFB staining and thinning of the cerebral cortex with shrunken cell bodies and pyknotic nuclei, indicating white matter and neuronal loss, respectively (A, Isch-PL, arrow, middle panel). Sections from the Isch-mAb group (A, arrow, right panel) show more healthy-appearing neurons compared with the Isch-PL brain section.

The global pathological scores for the hemi-brain sections (Fig. 3B) demonstrated that the scores in the Isch-PL group were higher indicating greater pathological damage compared with those in the Control and Isch-mAb groups (median, $P<0.05$). Although pathological injury to the gray and white matter, and parasagittal gray and white matter appeared to exhibit, lower pathological scores in the Isch-mAb group when compared with the Isch-PL group (Table 1), the differences did not achieve statistical significance. This result could potentially reflect our relatively small sample size, short-term reperfusion time after ischemia, and/or individual variability in the response to ischemia as determined by our pathological scoring system (Petersson et al., 2004).

3.2. Systemic infusions of anti-IL-1β-mAb decrease I/R-related apoptosis and caspase-3 activation

Fig. 4A contains representative sections in the Control (n=14), Isch-PL (n=14) and Isch-mAb (n=11) groups co-stained with ApopTag and NeuN. The arrows indicate the ApopTag positive cells, whereas arrowheads indicate the double-labeled ApopTag/NeuN positive cells (Fig. 4A, middle panel). The total Apop Tag stained cells were higher per area (mm^2) in the cerebral cortex of the placebo treated fetuses exposed to I/R (Isch-PL) than the in the Control fetal brains and the anti-IL-1β mAb I/R group (Isch-mAb, Fig. 4B, left panel, ANOVA, $F = 4.08$, $P<0.03$,). The number of double-labelled ApopTag and NeuN (ApopTag/NeuN) positive cells/mm^2 did not differ in the cerebral cortex among the study groups (ANOVA, $F = 2.21$, $P = 0.12$, Fig. 4B, middle panel). In contrast, the number of ApopTag positive cells that were not co-labeled with NeuN (ApopTag positive/non-neuronal cells)/mm^2 was significantly higher ($P<0.02$) in the Isch-PL than in the Control and Isch-mAb (4 B, right panel, ANOVA, $F = 4.59$, $P<0.02$). These findings demonstrate that systemic treatment with anti-IL-1β mAb infusions reduces I/R-related increases in apoptosis in non-neuronal cells.

Caspase-3 activity was measured by a DEVD-AFC cleavage assay and is an indicator of apoptosis. Caspase-3 activity was higher (P<0.03) in the Isch-PL (n=10) than in the Control (n=9) and Isch-mAb (n=10) treated groups (Fig. 5, ANOVA, $F = 44.4$, $P<0.001$). These findings suggest that systemic infusions of anti-IL-1β mAb result in significant reductions in

caspase-3 activity 24 h after exposure to I/R injury in ovine fetal brain. However, the anti-IL-1β mAb infusion resulted in a relatively modest decrease in caspase-3 activity.

3.3. Total ApopTag positive cells/mm^2 and ApopTag positive non-neuronal cells/mm^2 correlate with the global pathological injury scores

Correlational analysis showed that the total ApopTag positive cells/mm^2 (Fig. 6A, $r = 0.71$, n=21, $P<0.001$) and ApopTag/non-neuronal positive cells/mm^2 (Fig. 6B, $r = 0.78$, n=21, $P<0.001$) correlated positively with the global pathological scores (n=21) in the Isch-PL and Isch-mAb groups. These findings support the contention that assessment of brain injury by global pathological scoring correlates with cellular injury as determined by apoptosis.

3.4. Effects of systemic infusions of anti-IL-1β-mAb on I/R-related neuronal degeneration

Fig. 7A contains representative sections with FJB/NeuN positive stained cells in the Control (n=16), Isch-PL (n=13) and Isch-mAb (n=11) groups. Arrows indicate the FJB/NeuN stained positive cells. FJB/NeuN stained cells were higher (7 B, Kruskal-Wallis, $P<0.02$) in the Isch-PL than the Control group, and did not differ significantly between the in the Isch-mAb and Control (Kruskal-Wallis, $P>0.05$) or the Isch-PL and Isch-mAb (Kruskal-Wallis, $P>0.05$) groups. These findings suggest that 24 h after ischemic brain injury the number of dying/degenerating neurons (Rosen et al., 2006; Schmued et al., 1997; Schmued and Hopkins, 2000) increases in the fetal brain. However, the mAb did not have significant effects on this process. The lack of differences in the FJB/NeuN positive stained cells between the Isch-PL and Isch-mAb could potentially be a result of the high scatter in the Isch-PL group and the limited number of fetal sheep that we were able to study.

3.5. Systemic infusion of anti-IL-1β-mAb and I/R-related MBP and GFAP expression

Fig. 8A contains representative cerebral cortical sections from the Control (n=9), Isch-PL (n=12) and Isch-mAb (n=11) groups stained with anti-MBP mAb (MBP, top panel) and anti-GFAP pAb (GFAP, bottom panel). Computerized analysis of four randomly selected 8-bit grayscale images was used to quantify MBP and GFAP immunoreactive areas within the cerebral cortical fields. Differences were not observed in the amount of MBP-stained area per the field in the cerebral cortical sections among the study groups (Kruska-Wallis, $P=0.16$). Significant differences were found among the three study groups for anti-GFAP pAb-stained areas (Kruska-Wallis, $P<0.03$), but not for the ratio of MBP to GFAP (8 B, Kruska-Wallis, $P=0.09$). The analysis of multiple comparisons of mean ranks for the cerebral cortical sections showed that the area of GFAP immunoreactivity as a ratio to total field area was lower in the Isch-PL than in the Control group (Fig. 8, $P<0.03$). There were no differences in the area of GFAP immunoreactivity between Isch-mAb and Control ($P=0.54$, Fig. 8) or the Isch-PL and Isch-mAb groups ($P=0.46$, Fig. 8).

4. Discussion

The overall goal of the current study was to determine whether systemic intravenous infusions of anti-IL-1β mAb attenuate short-term I/R-related parenchymal injury in the ovine fetal brain. We studied the effects anti-IL-1β mAb infusions on injury to the fetal brain by examining histopathological injury, apoptosis, cerebral cortical neuronal degeneration

along with reactive gliosis and myelin basic protein expression in ovine fetuses at 85% of gestation. Cerebral ischemia was induced in the fetal sheep by ligation of the vertebral-occipital anastomoses and bilateral occlusion of the carotid arteries as previously reported (Williams et al., 1992). Although we have previously shown that infusions of anti-IL-1β mAb attenuated I/R-related BBB dysfunction (Chen et al., 2015), information regarding the effects of anti-IL-1 β mAb on parenchymal brain injury were not available in the fetus. The novel findings of the current study suggest that infusions of anti-IL-1β mAb 1) attenuate histopathological parenchymal brain injury; 2) reduce apoptosis in non-neuronal cells; and 3) decrease caspase 3 activity in the ovine fetal cerebral cortex 24 h after ischemia. Although the amount of neuroprotection provided by the anti-IL-1β mAb infusions was modest, the duration of reperfusion was only 24 h and, consequently, the amount of injury in the Isch-PL was relatively limited. Nonetheless, to the best of our knowledge, our findings are the first to show that any systemically administered mAb has the ability to exert neuroprotective effects on injury in the fetal brain.

I/R brain injury is one of the most severe neurologic conditions in the perinatal period (Vannucci and Hagberg, 2004), which may have its origins as *in utero* hypoxic/ischemic (HI) episodes resulting from antepartum or intrapartum events (Hill and Volpe, 1981). The pathological lesions caused by I/R brain are diverse during development and include multifocal ischemic injury in gray and white matter, which are most pronounced in the parasagittal regions (Huang and Castillo, 2008; Petersson et al., 2002; Reddy et al., 1998; Volpe, 1995). Neuropathological scoring provides an objective semi-quantitative assessment of brain lesions and has been used extensively in experimental and clinical studies of brain injury (Hoque et al., 2014). We used the scoring system of Williams *et al.* (Williams et al., 1992), which we modified to include scores for gray and white matter, as well as focal parasagittal gray and white matter (Petersson et al., 2002). In addition, we added a global score to assess the overall injury to entire hemi-brain section in the current study. The results of the histopathological examination suggested the systemic infusions of anti-IL-1β mAb attenuates injury based upon our global assessment of brain injury (Fig. 1). However, the anti-IL-1β mAb did not exert significant effects upon the regional pathological scores (Table 1). The possibility exists that if we had been able to examine a larger number of animals significant changes might have been detected in the gray and white matter regions (Table 1). Nonetheless, systemic treatment with anti-IL-1β mAb reduced the global pathological scores suggesting that systemic administration of this mAb could have neuroprotective effects on short-term injury in the developing brain. The findings that the number of apoptotic cells exhibit significant positive correlations with the global injury scores support the reliability of our scoring system (Fig. 6).

In addition to scoring the quantity of injury by neuropathological evaluation of LFB/H&E stained sections, we further characterized the lesions with immunohistochemical double staining using antibodies against GFAP and MBP (Petersson et al., 2002). Similar work has shown that infusions of neutralizing anti-TNFα mAb reduce cortical and subcortical injury and enhance cerebral blood flow after stroke in adult rats (Lavine et al., 1998). However, to the best of our knowledge, we have provided the first evidence to demonstrate that a therapeutic anti-inflammatory antibody, such as anti-IL-1β mAb, when given by the

clinically relevant intravenous route, attenuated parenchymal I/R-related brain injury in the developing fetal brain.

Apoptosis plays a pivotal role in neurodegeneration after I/R injury in the developing brain and caspase-3 activation is marker of cellular damage that contributes to apoptosis (Fatemi et al., 2009; Lavrik et al., 2005; Manabat et al., 2003; Nakajima et al., 2000). Our findings suggest that two doses of anti-IL-1β mAb given after ischemia reduced the number of cerebral cortical positive apoptotic cells and caspase-3 activity (Figs. 4 and 5). Nonetheless, it is important to point out that the effects of the anti-IL-1β mAb on caspase 3 activity were relatively modest.

The majority of the decreases in apoptosis appeared to occur in the non-neuronal population of cells rather than in neurons. The positive correlations between apoptosis and the global histopathological scores (Fig. 6) further suggest that the anti-IL-1β mAb-associated attenuation in short-term brain injury could in part have resulted from reduced non-neuronal apoptosis. Although neurons are the predominant cell population undergoing caspase-3-dependent apoptosis, caspase-3 activation can occur in a wide variety of cells including microglia, astrocytes, oligodendrocytes, infiltrated neutrophils, and mast cells (Dubey et al., 2016; Kavanagh et al., 2014; Manabat et al., 2003; Petito et al., 1998; Rossiter et al., 2002; Tzeng et al., 2013; Yoshikawa and Tasaka, 2003). Moreover, increases in IL-1β after I/R insults in brain are associated with activation of microglial and mast cells, and neutrophilic infiltration, which can facilitate apoptotic progression (Liu and McCullough, 2013). Therefore, the cellular effects of anti-IL-1β mAb treatment on the apoptosis and caspase-3 activity could affect numerous brain cell types, especially the immune cells, such as microglia, infiltrated neutrophils, and mast cells. The current findings are also consistent with our previous work in fetal sheep in which we observed that non-neuronal apoptosis represented the predominate form of apoptosis in the cerebral cortex of fetal sheep at both 70% and 90% of gestation (Malaeb et al., 2009). In addition, consistent with previous work in fetal sheep (Falkowski et al., 2002), the number of apoptotic cells that we observed after short-term ischemic brain injury were relatively limited. These findings could be a result of the mild injury observed after the 24 h recovery from ischemic brain injury.

We also attempted to analyze neuronal degeneration using FJB, which is a marker of neurons undergoing cell death and used double immunofluorescent staining for FJB and NeuN to assure that the FJB positive degenerating cells were in fact neurons. I/R was associated with increased FJB positive cells/mm^2 compared to the Control group. However, we were not able to detect a statically significant difference between the Isch-PL and the Isch-mAb groups most likely because of the high scatter in the Isch-PL group and the limited numbers of animals that could be studied in this large animal model.

I/R-related increases in IL-1β also result in damage to oligodendrocytes and reactive astrocytes during the perinatal period (Domowicz et al., 2011; Liu and McCullough, 2013; McClure et al., 2008; Sen and Levison, 2006; Svedin et al., 2007). Although we did not identify changes in MBP immunostaining or the ratio of MBP/GFAP 24 h after ischemia, we did detect a relative decrease in the amount of reactive astrocytes in the cerebral cortex as suggested by the decrease in the percent of the section occupied by GFAP immunoreactivity

in the Isch-PL treated compared with the Control group (Fig. 8). These findings are in contrast to our former work in which the ratio of MBP to GFAP was decreased 48 and 72 h after a similar insult (Petersson et al., 2002). The differences between our current study and former work are most likely a result of differences in the relative duration of reperfusion because the period of ischemia and the gestational ages of the fetal sheep were similar between the two studies (Petersson et al., 2002). Moreover, in the current study, we have examined cerebral cortical sections rather than specifically white matter (Petersson et al., 2002). Future work would need to examine specific markers of white matter injury to determine if treatment with anti-IL-1β mAb has protective effects on oligodendrocyte damage after I/R injury.

Consistent with our findings of reduced immunohistochemical expression of GFAP (Fig. 8), damage to astrocytes has also been reported in fetal sheep at 70% of gestation that were exposed to umbilical cord occlusion (Mallard et al., 2003). Similarly, Sullivan *et al.*, demonstrated in neonatal pigs that HI resulted in decreases in the average astrocyte size, and the number and length of astrocyte processes in all cortical layers as early as eight hours after the insult (Sullivan et al., 2010b). Moreover, it is thought that an initial reduction in astrocytes is detrimental to the neuronal survival, but that later astroglial proliferation is an adaptive response in order to replace lost brain tissue and re-establish neuronal-glial connectivity in cortex (Sullivan et al., 2010a, b). However, differences in the percent area of the astrocytic immunoreactivity were not detected between the Isch-PL and the anti-IL-1β mAb treated ischemic groups.

In our previous work, we have shown that systemically administered anti-IL-1β mAb penetrated into the fetal brain, attenuated I/R-related increases in the expression of IL-1β protein, attenuated non-specific BBB dysfunction and reduced IL-1β protein transport across the BBB (Chen et al., 2015; Patra et al., 2017). However, direct evidence for the beneficial effects of anti-IL-1β mAb treatment on actual I/R-related brain tissue injury was lacking until our present work. Therefore, in addition to the protective effects of systemic intravenous infusions of anti-IL-1β mAb on BBB function in the fetal brain, intravenous administration of modest doses of anti-IL-1β mAb also attenuate short-term parenchymal tissue damage to the fetal brain after ischemia.

The precise mechanism(s) by which the systemic intravenous infusions of anti-IL-1β mAb attenuate the short-term parenchymal tissue injury after I/R in the fetal brain remains to be determined. However, several possibilities exist. The anti-IL-1β mAb could potentially exert its beneficial effects on the fetal brain parenchyma by reducing non-specific transport of potentially damaging molecules across the BBB (Chen et al., 2015), reducing IL-1β transport across the BBB (Patra et al., 2017), and/or by reducing IL-1β protein levels within the fetal brain (Chen et al., 2015). Alternatively, direct penetration of the anti-IL-1β mAb into the brain parenchyma could attenuate IL-1β mediated generalized parenchymal inflammation (Chen et al., 2015). In addition, IL-1β neutralization by the mAb could also modulate the function of cells within the neurovascular unit (Abbott, 2000), thereby reducing the transmission of other inflammatory signals into the brain parenchyma. This could then further attenuate the spread of other inflammatory signals within the brain.

There are several limitations to our study as well as potential opportunities for future study. In the current study, we administered the anti-IL-1β mAb 15 min after the end of the bilateral carotid artery occlusion as a proof of principle. However, such a paradigm is not clinically feasible. Therefore, in order for treatment with the anti-IL-1β mAb to have translational potential, additional studies are required to examine the effect of delayed mAb treatment with longer periods of reperfusion after ischemia. In addition, the potential impact of mAb treatment on immunity would also need to be determined. It would also be of interest to determine the effect of the mAb infusions on the ECoG signal. However, we unfortunately are not able to monitor the fetal the ECoG signal continuously in our fetal sheep, therefore we mainly use the fetal the ECoG signal to determine that our 30 min ischemic insult would is adequate (Chen et al., 2015; Gunn et al., 1997). Therefore, we are not able comment on potential effects of the mAbs on the continuous ECoG signal. We examined white matter integrity with LFB/H&E staining and MBP. Although we have previously shown an abundance of myelin in the fetal sheep brain at the same time in gestation and that ischemia with reperfusion for 48 and 72 h resulted in a dramatic reduction in immunocytochemically detectable MBP (Petersson et al., 2002), it would also be of great interest to examine earlier markers of myelin integrity in this model. In addition, GFAP and MBP were assessed on residual frozen cerebral cortical tissue. It would have been more optimal to evaluate GFAP and MBP in pre-defined brain regions. Although we did not study microglia activation in our current study, this is also an important area of investigation for future studies in the context of our study paradigm.

5. Conclusions

I/R insults are known to trigger inflammation in the immature brain (Ferriero, 2004). Critical phases of inflammation are regulated by multiple mediators including cytokines and chemokines, leading to BBB dysfunction, brain tissue pathological injury, and cellular degeneration and death. In the present study, we demonstrated the neuroprotective effects of anti-IL-1β mAb on short-term I/R-related brain tissue injury by demonstrating that the anti-IL-1β mAb attenuated parenchymal brain injury and cellular apoptosis. These findings strongly support the concept that secondary inflammation contributes to perinatal brain injury.

Acknowledgments

Abbreviations

BBB   blood-brain barrier

| **GFAP** | glial fibrillary acidic protein |
HI	hypoxic-ischemic
IL-1β	interleukin-1β
I/R	hypoxic-ischemia/reperfusion
mAb	monoclonal antibody

References

Abbott NJ. Inflammatory mediators and modulation of blood-brain barrier permeability. Cellular and molecular neurobiology. 2000; 20:131–147. [PubMed: 10696506]

Back SA. Perinatal white matter injury: the changing spectrum of pathology and emerging insights into pathogenetic mechanisms. Ment Retard Dev Disabil Res Rev. 2006; 12:129–140. [PubMed: 16807910]

Bartha AI, Foster-Barber A, Miller SP, Vigneron DB, Glidden DV, Barkovich AJ, Ferriero DM. Neonatal encephalopathy: association of cytokines with MR spectroscopy and outcome. Pediatric research. 2004; 56:960–966. [PubMed: 15496611]

Bhalala US, Koehler RC, Kannan S. Neuroinflammation and neuroimmune dysregulation after acute hypoxic-ischemic injury of developing brain. Front Pediatr. 2014; 2:144. [PubMed: 25642419]

Bose CL, Laughon MM, Allred EN, O'Shea TM, Van Marter LJ, Ehrenkranz RA, Fichorova RN, Leviton A. Systemic inflammation associated with mechanical ventilation among extremely preterm infants. Cytokine. 2013; 61:315–322. [PubMed: 23148992]

Brown AW, Brierley JB. Anoxic-ischaemic cell change in rat brain light microscopic and fine-structural observations. J Neurol Sci. 1972; 16:59–84. [PubMed: 5034855]

Carty ML, Wixey JA, Colditz PB, Buller KM. Post-insult minocycline treatment attenuates hypoxia-ischemia-induced neuroinflammation and white matter injury in the neonatal rat: a comparison of two different dose regimens. International journal of developmental neuroscience: the official journal of the International Society for Developmental Neuroscience. 2008; 26:477–485. [PubMed: 18387771]

Chen X, Sadowska GB, Zhang J, Kim JE, Cummings EE, Bodge CA, Lim YP, Makeyev O, Besio WG, Gaitanis J, Threlkeld SW, Banks WA, Stonestreet BS. Neutralizing anti-interleukin-1beta antibodies modulate fetal blood-brain barrier function after ischemia. Neurobiol Dis. 2015; 73:118–129. [PubMed: 25258170]

Chen X, Threlkeld SW, Cummings EE, Juan I, Makeyev O, Besio WG, Gaitanis J, Banks WA, Sadowska GB, Stonestreet BS. Ischemia–reperfusion impairs blood–brain barrier function and alters tight junction protein expression in the ovine fetus. Neuroscience. 2012; 226:89–100. [PubMed: 22986172]

Chen X, Threlkeld SW, Cummings EE, Sadowska GB, Lim YP, Padbury JF, Sharma S, Stonestreet BS. In-vitro Validation of Cytokine Neutralizing Antibodies by Testing with Ovine Mononuclear Splenocytes. Journal of Comparative Pathology. 2013; 148:252–258. [PubMed: 22819013]

Chew LJ, Takanohashi A, Bell M. Microglia and inflammation: impact on developmental brain injuries. Ment Retard Dev Disabil Res Rev. 2006; 12:105–112. [PubMed: 16807890]

Chung CS, Song GY, Moldawer LL, Chaudry IH, Ayala A. Neither Fas ligand nor endotoxin is responsible for inducible peritoneal phagocyte apoptosis during sepsis/peritonitis. J Surg Res. 2000; 91:147–153. [PubMed: 10839964]

Domowicz MS, Henry JG, Wadlington N, Navarro A, Kraig RP, Schwartz NB. Astrocyte precursor response to embryonic brain injury. Brain Res. 2011; 1389:35–49. [PubMed: 21396923]

Dubey M, Nagarkoti S, Awasthi D, Singh AK, Chandra T, Kumaravelu J, Barthwal MK, Dikshit M. Nitric oxide-mediated apoptosis of neutrophils through caspase-8 and caspase-3-dependent mechanism. Cell Death & Disease. 2016; 7:e2348. [PubMed: 27584786]

Elitt CM, Sadowska GB, Stopa EG, Pinar H, Petersson KH, Stonestreet BS. Effects of antenatal steroids on ischemic brain injury in near-term ovine fetuses. Early Hum Dev. 2003; 73:1–15. [PubMed: 12932889]

Falkowski A, Hammond R, Han V, Richardson B. Apoptosis in the preterm and near term ovine fetal brain and the effect of intermittent umbilical cord occlusion. Brain research. 2002; 136:165–173. [PubMed: 12101033]

Fatemi A, Wilson MA, Johnston MV. Hypoxic-ischemic encephalopathy in the term infant. Clinics in perinatology. 2009; 36:835–858. vii. [PubMed: 19944838]

Ferriero DM. Neonatal brain injury. N Engl J Med. 2004; 351:1985–1995. [PubMed: 15525724]

Gunn AJ, Gunn TR, de Haan HH, Williams CE, Gluckman PD. Dramatic neuronal rescue with prolonged selective head cooling after ischemia in fetal lambs. The Journal of Clinical Investigation. 1997; 99:248–256. [PubMed: 9005993]

Hill A, Volpe JJ. Seizures, hypoxic-ischemic brain injury, and intraventricular hemorrhage in the newborn. Annals of neurology. 1981; 10:109–121. [PubMed: 7283398]

Hoque N, Sabir H, Maes E, Bishop S, Thoresen M. Validation of a neuropathology score using quantitative methods to evaluate brain injury in a pig model of hypoxia ischaemia. J Neurosci Methods. 2014; 230:30–36. [PubMed: 24747875]

Huang BY, Castillo M. Hypoxic-ischemic brain injury: imaging findings from birth to adulthood. Radiographics. 2008; 28:417–439. quiz 617. [PubMed: 18349449]

Kavanagh E, Rodhe J, Burguillos MA, Venero JL, Joseph B. Regulation of caspase-3 processing by cIAP2 controls the switch between pro-inflammatory activation and cell death in microglia. Cell Death Dis. 2014; 5:e1565. [PubMed: 25501826]

Lan KM, Tien LT, Pang Y, Bhatt AJ, Fan LW. IL-1 receptor antagonist attenuates neonatal lipopolysaccharide-induced long-lasting learning impairment and hippocampal injury in adult rats. Toxicology letters. 2015; 234:30–39. [PubMed: 25665855]

Lavine SD, Hofman FM, Zlokovic BV. Circulating antibody against tumor necrosis factor-alpha protects rat brain from reperfusion injury. J Cereb Blood Flow Metab. 1998; 18:52–58. [PubMed: 9428305]

Lavrik IN, Golks A, Krammer PH. Caspases: pharmacological manipulation of cell death. J Clin Invest. 2005; 115:2665–2672. [PubMed: 16200200]

Leonardo CC, Pennypacker KR. Neuroinflammation and MMPs: potential therapeutic targets in neonatal hypoxic-ischemic injury. Journal of neuroinflammation. 2009; 6:13. [PubMed: 19368723]

Liu F, McCullough LD. Inflammatory responses in hypoxic ischemic encephalopathy. Acta Pharmacol Sin. 2013; 34:1121–1130. [PubMed: 23892271]

Liu J, Feng ZC. Increased umbilical cord plasma interleukin-1 beta levels was correlated with adverse outcomes of neonatal hypoxic-ischemic encephalopathy. J Trop Pediatr. 2010; 56:178–182. [PubMed: 19822562]

Malaeb SN, Hovanesian V, Sarasin MD, Hartmann SM, Sadowska GB, Stonestreet BS. Effects of maternal antenatal glucocorticoid treatment on apoptosis in the ovine fetal cerebral cortex. J Neurosci Res. 2009; 87:179–189. [PubMed: 18711727]

Mallard C, Welin AK, Peebles D, Hagberg H, Kjellmer I. White matter injury following systemic endotoxemia or asphyxia in the fetal sheep. Neurochem Res. 2003; 28:215–223. [PubMed: 12608695]

Manabat C, Han BH, Wendland M, Derugin N, Fox CK, Choi J, Holtzman DM, Ferriero DM, Vexler ZS. Reperfusion differentially induces caspase-3 activation in ischemic core and penumbra after stroke in immature brain. Stroke. 2003; 34:207–213. [PubMed: 12511776]

Martin D, Chinookoswong N, Miller G. The Interleukin-1 Receptor Antagonist (rhIL-1ra) Protects against Cerebral Infarction in a Rat Model of Hypoxia-Ischemia. Experimental neurology. 1994; 130:362–367. [PubMed: 7867766]

McAdams RM, Juul SE. The role of cytokines and inflammatory cells in perinatal brain injury. Neurol Res Int. 2012; 2012:561494. [PubMed: 22530124]

McClure MM, Riddle A, Manese M, Luo NL, Rorvik DA, Kelly KA, Barlow CH, Kelly JJ, Vinecore K, Roberts CT, Hohimer AR, Back SA. Cerebral blood flow heterogeneity in preterm sheep: lack

of physiologic support for vascular boundary zones in fetal cerebral white matter. J Cereb Blood Flow Metab. 2008; 28:995–1008. [PubMed: 18091757]

Nakajima W, Ishida A, Lange MS, Gabrielson KL, Wilson MA, Martin LJ, Blue ME, Johnston MV. Apoptosis has a prolonged role in the neurodegeneration after hypoxic ischemia in the newborn rat. J Neurosci. 2000; 20:7994–8004. [PubMed: 11050120]

Newacheck PW, Taylor WR. Childhood chronic illness: prevalence, severity, and impact. American journal of public health. 1992; 82:364–371. [PubMed: 1536351]

Oygur N, Sonmez O, Saka O, Yegin O. Predictive value of plasma and cerebrospinal fluid tumour necrosis factor-alpha and interleukin-1 beta concentrations on outcome of full term infants with hypoxic-ischaemic encephalopathy. Arch Dis Child Fetal Neonatal Ed. 1998; 79:F190–193. [PubMed: 10194989]

Patra A, Chen X, Sadowska GB, Zhang J, Lim YP, Padbury JF, Banks WA, Stonestreet BS. Neutralizing anti-interleukin-1beta antibodies reduce ischemia-related interleukin-1beta transport across the blood-brain barrier in fetal sheep. Neuroscience. 2017; 346:113–125. [PubMed: 28089577]

Petersson KH, Pinar H, Stopa EG, Faris RA, Sadowska GB, Hanumara RC, Stonestreet BS. White matter injury after cerebral ischemia in ovine fetuses. Pediatric research. 2002; 51:768–776. [PubMed: 12032276]

Petersson KH, Pinar H, Stopa EG, Sadowska GB, Hanumara RC, Stonestreet BS. Effects of exogenous glucose on brain ischemia in ovine fetuses. Pediatric research. 2004; 56:621–629. [PubMed: 15319457]

Petito CK, Olarte JP, Roberts B, Nowak TS Jr, Pulsinelli WA. Selective glial vulnerability following transient global ischemia in rat brain. J Neuropathol Exp Neurol. 1998; 57:231–238. [PubMed: 9600215]

Pharoah PO. The epidemiology of chronic disability in childhood. International rehabilitation medicine. 1985; 7:11–17. [PubMed: 3157653]

Reddy K, Mallard C, Guan J, Marks K, Bennet L, Gunning M, Gunn A, Gluckman P, Williams C. Maturational change in the cortical response to hypoperfusion injury in the fetal sheep. Pediatric research. 1998; 43:674–682. [PubMed: 9585015]

Relton JK, Martin D, Thompson RC, Russell DA. Peripheral administration of Interleukin-1 Receptor antagonist inhibits brain damage after focal cerebral ischemia in the rat. Experimental neurology. 1996; 138:206–213. [PubMed: 8620919]

Rosen GD, Mesples B, Hendriks M, Galaburda AM. Histometric changes and cell death in the thalamus after neonatal neocortical injury in the rat. Neuroscience. 2006; 141:875–888. [PubMed: 16725276]

Rossiter JP, Anderson LL, Yang F, Cole GM. Caspase-3 activation and caspase-like proteolytic activity in human perinatal hypoxic-ischemic brain injury. Acta Neuropathol. 2002; 103:66–73. [PubMed: 11841033]

Rothel JS, Hurst L, Seow HF, Pépin M, Berthon P, Corner LA, Wood PR. Analysis of ovine IL-1 beta production in vivo and in vitro by enzyme immunoassay and immunohistochemistry. Vet Immunol Immunopathol. 1997; 57:267–278. [PubMed: 9261964]

Sadowska GB, Chen X, Zhang J, Lim YP, Cummings EE, Makeyev O, Besio WG, Gaitanis J, Padbury JF, Banks WA, Stonestreet BS. Interleukin-1beta transfer across the blood-brain barrier in the ovine fetus. J Cereb Blood Flow Metab. 2015; 35:1388–1395. [PubMed: 26082012]

Savard A, Brochu ME, Chevin M, Guiraut C, Grbic D, Sebire G. Neuronal self-injury mediated by IL-1beta and MMP-9 in a cerebral palsy model of severe neonatal encephalopathy induced by immune activation plus hypoxia-ischemia. Journal of neuroinflammation. 2015; 12:111. [PubMed: 26025257]

Savard A, Lavoie K, Brochu ME, Grbic D, Lepage M, Gris D, Sebire G. Involvement of neuronal IL-1beta in acquired brain lesions in a rat model of neonatal encephalopathy. Journal of neuroinflammation. 2013; 10:110. [PubMed: 24007297]

Schmued LC, Albertson C, Slikker W Jr. Fluoro-Jade: a novel fluorochrome for the sensitive and reliable histochemical localization of neuronal degeneration. Brain Res. 1997; 751:37–46. [PubMed: 9098566]

Schmued LC, Hopkins KJ. Fluoro-Jade B: a high affinity fluorescent marker for the localization of neuronal degeneration. Brain Res. 2000; 874:123–130. [PubMed: 10960596]

Sen E, Levison SW. Astrocytes and developmental white matter disorders. Ment Retard Dev Disabil Res Rev. 2006; 12:97–104. [PubMed: 16807889]

Seow HF, Rothel JS, Wood PR. Expression and purification of recombinant ovine interleukin-1 beta from Escherichia coli. Vet Immunol Immunopathol. 1994; 41:229–239. [PubMed: 7941306]

Silverstein FS, Barks JD, Hagan P, Liu XH, Ivacko J, Szaflarski J. Cytokines and perinatal brain injury. Neurochem Int. 1997; 30:375–383. [PubMed: 9106251]

Stanley FJ. The aetiology of cerebral palsy. Early Hum Dev. 1994; 36:81–88. [PubMed: 8200323]

Stoll BJ, Hansen NI, Adams-Chapman I, Fanaroff AA, Hintz SR, Vohr B, Higgins RD. National Institute of Child H, Human Development Neonatal Research N. Neurodevelopmental and growth impairment among extremely low-birth-weight infants with neonatal infection. Jama. 2004; 292:2357–2365. [PubMed: 15547163]

Stonestreet BS, Petersson KH, Sadowska GB, Pettigrew KD, Patlak CS. Antenatal steroids decrease blood-brain barrier permeability in the ovine fetus. Am J Physiol. 1999; 276:R283–289. [PubMed: 9950903]

Sullivan SM, Bjorkman ST, Miller SM, Colditz PB, Pow DV. Morphological changes in white matter astrocytes in response to hypoxia/ischemia in the neonatal pig. Brain Res. 2010a; 1319:164–174. [PubMed: 20079338]

Sullivan SM, Bjorkman ST, Miller SM, Colditz PB, Pow DV. Structural remodeling of gray matter astrocytes in the neonatal pig brain after hypoxia/ischemia. Glia. 2010b; 58:181–194. [PubMed: 19606499]

Svedin P, Guan J, Mathai S, Zhang R, Wang X, Gustavsson M, Hagberg H, Mallard C. Delayed peripheral administration of a GPE analogue induces astrogliosis and angiogenesis and reduces inflammation and brain injury following hypoxia-ischemia in the neonatal rat. Developmental neuroscience. 2007; 29:393–402. [PubMed: 17762207]

Tang M, Alexander H, Clark RS, Kochanek PM, Kagan VE, Bayir H. Minocycline reduces neuronal death and attenuates microglial response after pediatric asphyxial cardiac arrest. J Cereb Blood Flow Metab. 2010; 30:119–129. [PubMed: 19756023]

Ten VS, Starkov A. Hypoxic-ischemic injury in the developing brain: the role of reactive oxygen species originating in mitochondria. Neurol Res Int. 2012; 2012:542976. [PubMed: 22548167]

Tzeng TT, Tsay HJ, Chang L, Hsu CL, Lai TH, Huang FL, Shiao YJ. Caspase 3 involves in neuroplasticity, microglial activation and neurogenesis in the mice hippocampus after intracerebral injection of kainic acid. J Biomed Sci. 2013; 20:90. [PubMed: 24313976]

Vannucci RC. Hypoxic-ischemic encephalopathy. Am J Perinatol. 2000; 17:113–120. [PubMed: 11012134]

Vannucci SJ, Hagberg H. Hypoxia-ischemia in the immature brain. J Exp Biol. 2004; 207:3149–3154. [PubMed: 15299036]

Volpe, J. Neurology of the Newborn. WB Saunders; Philadelphia, PA: 1995. Hypoxic-ischemic encephalopathy; p. 260-313.

Walsh MC, Morris BH, Wrage LA, Vohr BR, Poole WK, Tyson JE, Wright LL, Ehrenkranz RA, Stoll BJ, Fanaroff AA. National Institutes of Child H, Human Development Neonatal Research N. Extremely low birthweight neonates with protracted ventilation: mortality and 18-month neurodevelopmental outcomes. J Pediatr. 2005; 146:798–804. [PubMed: 15973322]

Williams CE, Gunn AJ, Mallard C, Gluckman PD. Outcome after ischemia in the developing sheep brain: an electroencephalographic and histological study. Annals of neurology. 1992; 31:14–21. [PubMed: 1543346]

Wood PR, Rothel JS, McWaters PG, Jones SL. Production and characterization of monoclonal antibodies specific for bovine gamma-interferon. Vet Immunol Immunopathol. 1990; 25:37–46. [PubMed: 2112286]

Yoshikawa H, Tasaka K. Caspase-dependent and -independent apoptosis of mast cells induced by withdrawal of IL-3 is prevented by Toll-like receptor 4-mediated lipopolysaccharide stimulation. Eur J Immunol. 2003; 33:2149–2159. [PubMed: 12884289]

- Anti-IL-1β mAbs attenuate short-term fetal parenchymal brain injury after ischemia

- Anti-IL-1β mAbs decrease ischemia-related apoptosis and caspase-3 activity

- Findings suggest that secondary inflammation contributes to perinatal brain injury
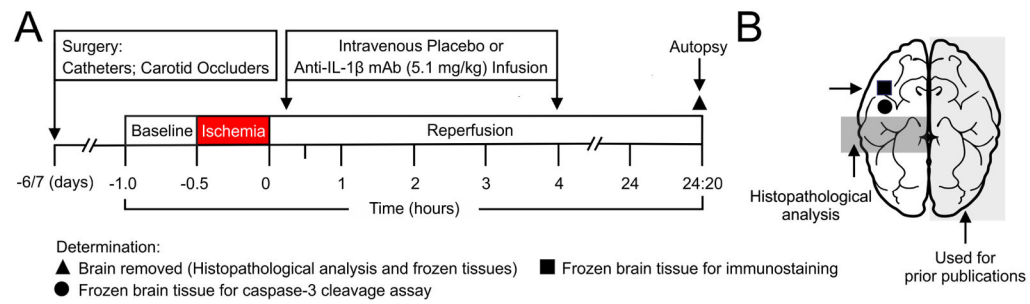
Fig. 1.

A. Study design. Surgical preparation was 6–7 days before the onset of the studies. After the baseline determinations, ischemia was induced for 30 min by inflation of the bilateral carotid artery occluders. At the end of ischemia, the occluders were deflated and reperfusion continued for 24 h and 20 min. In the sham operated Control sheep, the occluders were not inflated. Placebo (0.154 M NaCl) or anti-IL-1β mAb (5.1 mg/kg) was infused intravenously into the fetus 15 min and 4 h after the end of ischemia. Each infusion was performed over 2 H. At the end of the studies, the ewe and fetus were sacrificed with intravenous pentobarbital (100–200 mg/kg). The brain removed for analysis.

B. Schematic depiction of the sheep brain dissection. The shaded light gray half of the brain had been used for our prior studies (Chen et al., 2015; Patra et al., 2017). The shaded dark gray coronal section from the contralateral brain were obtained at the level of the hypothalamus (mammillary bodies) and used for histopathological analysis (LFB/H&E staining) in the current study. The residual brain tissue was immediately frozen in liquid nitrogen and remained at −80ºC until analysis. The black square indicates the section of the cerebral cortex that was obtained for the immunohistochemical analysis that included the FJB/NeuN, ApopTag/NeuN, and GFAP and MBP staining. The black circle shows the frozen tissue obtained for the caspase-3 cleavage assay.

| Control	Isch-PL	Isch-mAb
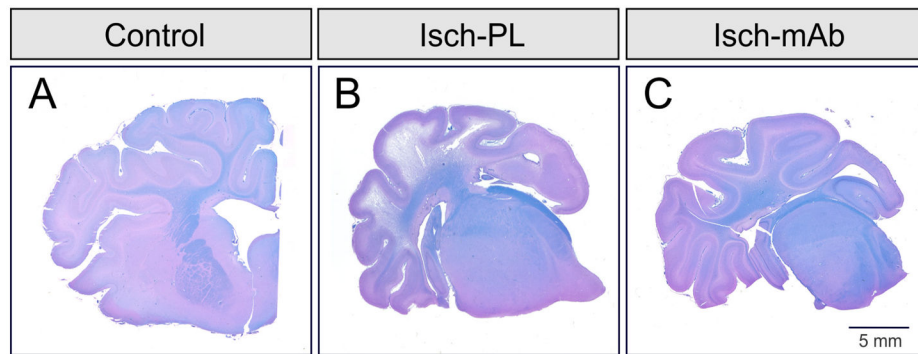
Fig. 2.
A. Representative coronal hemi-brain section at the level of the hypothalamus (mammillary bodies) from a sham Control fetal sheep stained with Luxol fast blue-hematoxylin and eosin. The control brain exhibits homogenous blue stained myelin and healthy appearing cerebral cortex. This is a score of zero.
**B.** Coronal hemi-brain section from an Isch-PL treated fetal sheep stained with Luxol fast blue-hematoxylin and eosin. The section from the Isch-PL group shows a shrunken cerebral cortical section with decreased blue staining indicating white matter loss and marked thinning of the cerebral cortex indicating neuronal loss. This represents a score of 4.
C. Coronal hemi-brain section from an Isch-mAb treated fetal sheep stained with Luxol fast blue-hematoxylin and eosin. The section from the Isch-mAb group shows more of the blue stained myelin suggesting relative preservation of the white matter and comparative preservation of the cerebral cortex. This represents a score of one. These findings suggest that systemic intravenous infusions of anti-IL-1β mAb have beneficial neuroprotective effects on short-term brain injury in the ovine fetus.
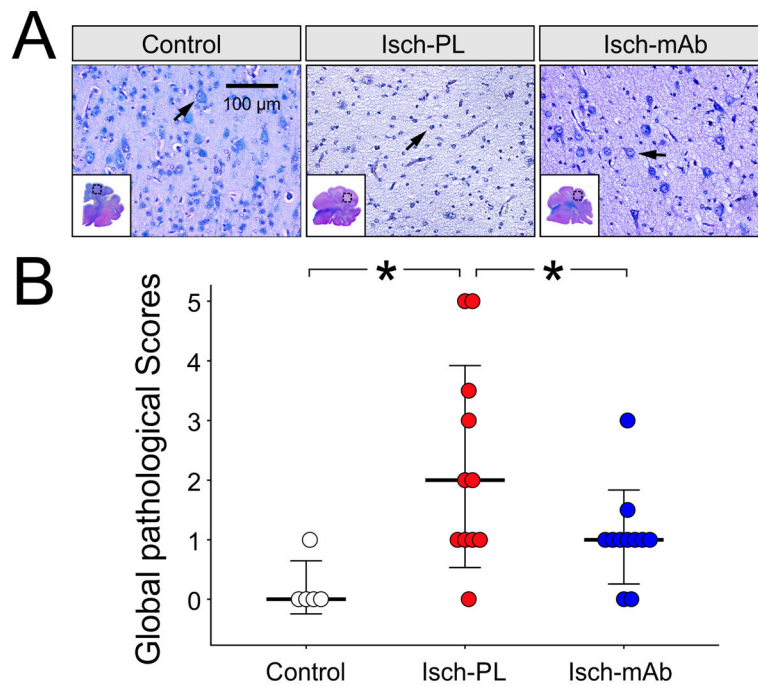
Fig. 3.

A. Brain sections stained with LFB/H&E from control fetuses, placebo-treated fetuses exposed to bilateral carotid artery occlusion followed by 24 h of reperfusion (Isch-PL), and anti-IL-1β mAb-infused fetuses exposed to carotid occlusion and 24 h of reperfusion (Isch-mAb). The histological panels shown are representative of the mean scores shown in 3B. Sections from the Control fetus exhibited healthy appearing neurons (arrow) and white matter with homogenously blue-stained myelin. This represents a score of 0. In contrast, sections from the Isch-PL fetuses exhibited severe neuronal loss with numerous shrunken pyknotic neurons (arrow), and extensive white matter loss, manifested by marked pallor on LFB/H&E staining. This represents a score of 3. The sections from Isch-mAb group showed healthy appearing cortex with normal-appearing neurons (arrow). This represents a score of 1.

B. Global pathological scores for brain damage in the Control (n = 5), Isch-PL (n =11), and Isch-mAb (n = 12) groups are shown. All sections received global pathological ischemia scores of 0–5, where 0 = 0%, 1 = 1–25%, 2 = 26–50%, 3 = 51–75%, 4 = 76–95%, and 5 = 96–100% of the area damaged. Scored values are shown as dot-density plots with the median value and standard deviation (SD) shown in bars. Global pathological scores were higher in the Isch-PL than in the Control and Isch-mAb groups. $*P < 0.05$ vs Isch- PL.
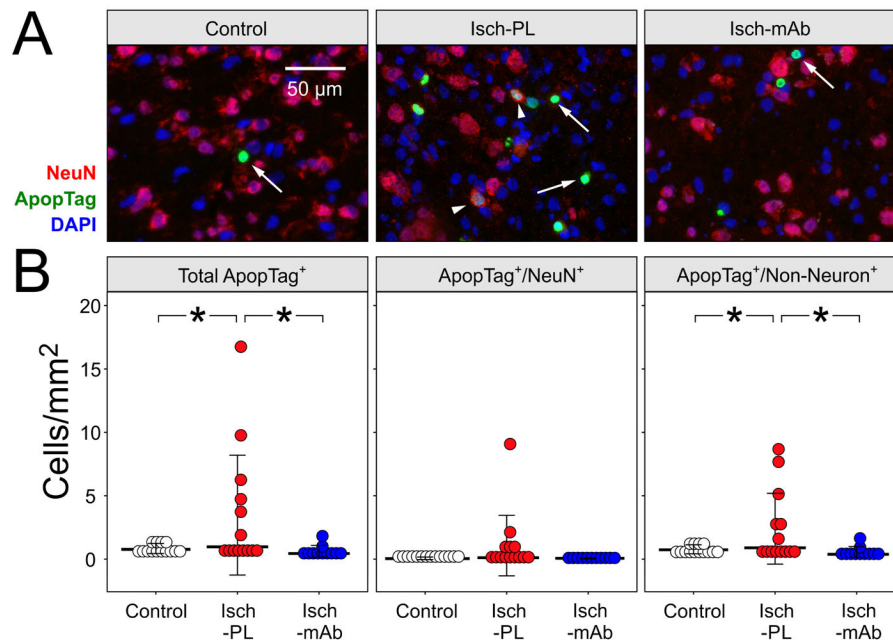
Fig. 4.
A. Representative cerebral cortical cryosections show double immunofluorescent staining of ApopTag (green) and NeuN (red) in the Control (n=14), Isch-PL (n=14), and Isch-mAb (n=11) study groups. DAPI (blue) is used as counterstain. ApopTag$^+$ cells are indicated with arrows and co-staining of ApopTag$^+$/NeuN$^+$ cells are indicated with arrowheads.
B. Dot-density plots with median value and SD bars were obtained for quantification of the total ApopTag$^+$ (left), ApopTag$^+$/NeuN$^+$ (middle), and ApopTag$^+$/Non-Neuronal$^+$ (right) cells/mm^2 in the Control, Isch-PL, and Isch-mAb groups. The total ApopTag$^+$ (ANOVA, $P<0.03$) and ApopTag$^+$/Non-Neuronal$^+$ (ANOVA, $P<0.02$) cells were higher in the Isch-PL than in the Control and Isch-mAb treated groups, but ApopTag$^+$/NeuN$^+$ cells did not differ among the three groups.
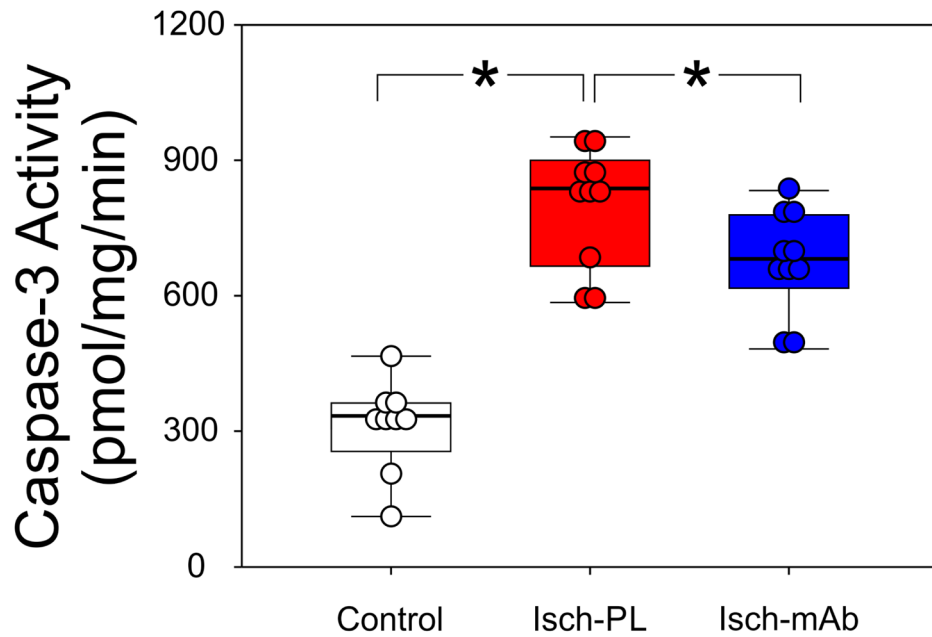
Fig. 5.
DEVD-AFC assays were performed on cerebral cortical homogenates obtained from the Control (n=9), Isch-PL (n=10), and Isch-mAb (n=10) study groups. AFC was used to obtain a standard curve and caspase 3 activities were expressed as picomoles per milligram protein per minute (pmol/mg/min). *P<0.05. Caspase 3 activity was higher in the cerebral cortex of the placebo treated fetal sheep exposed to 24 h I/R injury (Isch-PL group) than in the Control and Isch-mAb treated groups. However, the magnitude of the differences between the Isch-PL and Isch-mAb treated groups were relatively small.
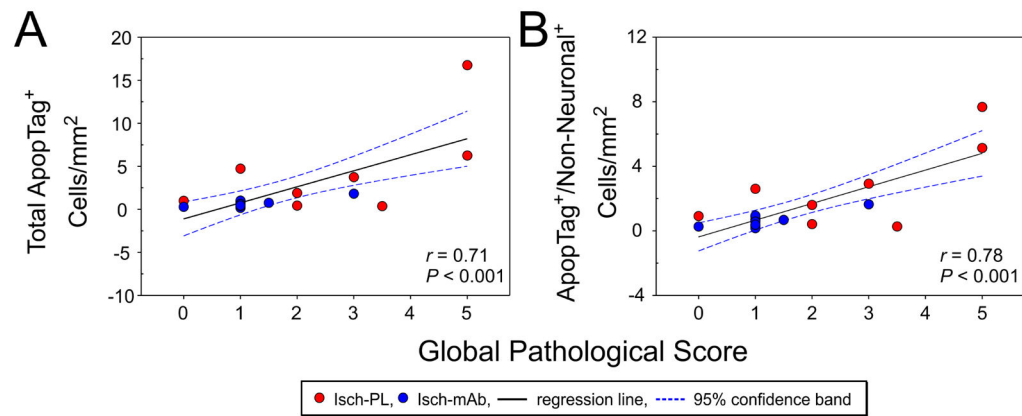
Fig. 6.
A. Linear regression analysis shows a positive correlation between total ApopTag$^+$ cells/mm^2 and the global pathological scores ($r = 0.71$, n=21, $P < 0.001$) in the Isch-PL (red circles) and Isch-mAb (blue circles) study groups. Regression lines (black line) and 95% confidence band (blue dashed line). Linear regression analysis shows a positive correlation between ApopTag$^+$/Non-Neuronal$^+$ cells/mm^2 and the global pathological scores ($r = 0.78$, n=21, $P < 0.001$) in the Isch-PL (red circles) and Isch-mAb (blue circles) groups. Regression lines (black line) and 95% confidence band (blue dashed line).
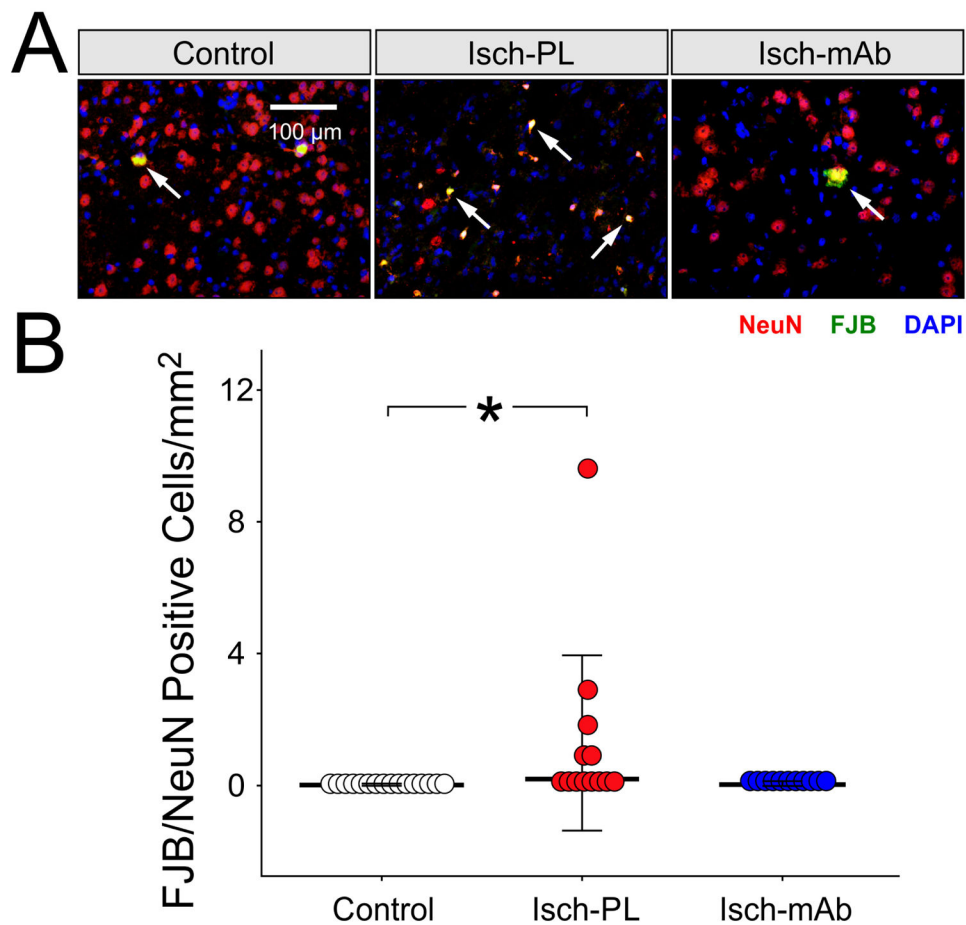
Fig. 7.
A. Representative cerebral cortical sections from Control (n=16), Isch-PL (n=13), and Isch-mAb (n=11) groups stained with FJB (green), anti-NeuN mAb (red), and Dapi (blue) are shown. Arrows indicate FJB/anti-NeuN mAb double stained yellow cells.
B. The number of FJB/NeuN positive cells per counting field area (mm^2) is plotted as a dot-density plot with median values and SD bars. The number of FJB/NeuN positive cells per counting field area was higher in the Isch-PL than in the Control group (Kruskal-Wallis, $P<0.02$), but did not differ between the Control and Isch-mAb or the Isch-PL and Isch-mAb groups (Kruskal-Wallis, $P>0.05$) groups.
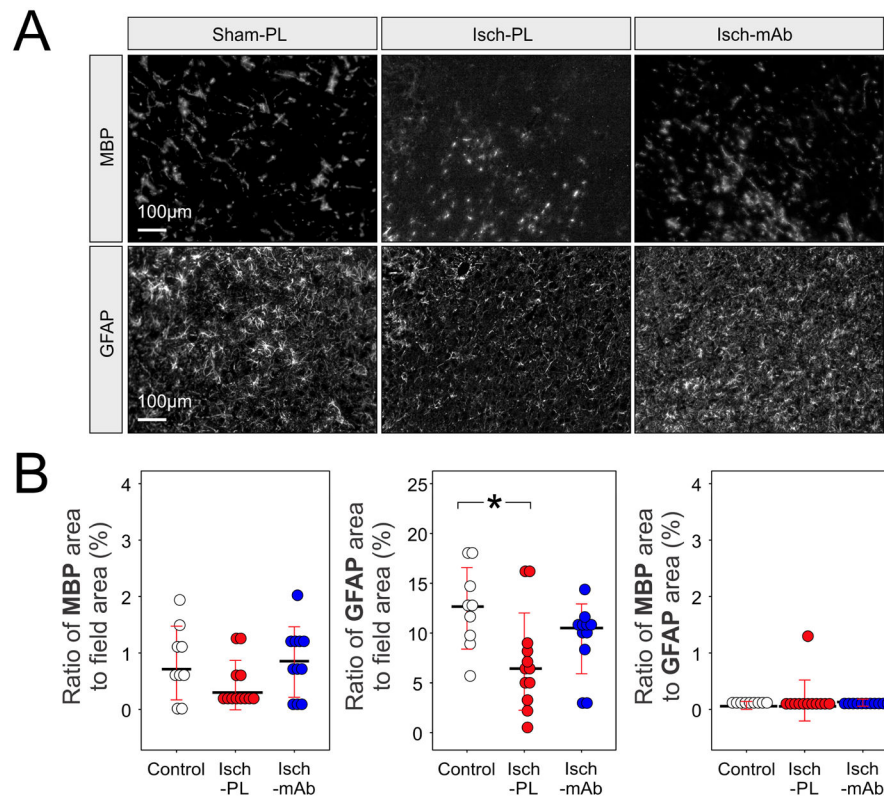
Fig. 8.

A. Grayscale images showing the cerebral cortical sections from the Control fetuses (Control, n=9) subjected to 30 min of ischemia and 24 h of reperfusion (I/R) treated with placebo (Isch-PL, n=12) or anti-IL-1β mAb (Isch-mAb, n=11). The cerebral cortical sections were stained with anti-MBP mAb (MBP, top panel) and anti-GFAP pAb (GFAP, bottom panel). Differences were not observed in the amount of MBP-stained per the field area in the cerebral cortical sections among the study groups. However, the sections from Isch-PL group exhibited decreased immunoreactivity for GFAP compared with the Control group. The sections from Control and Isch-mAb groups appeared to have more enlarged and densely stained areas of GFAP. This suggests that immunohistochemical expression of GFAP was reduced in the fetal cerebral cortex after short-term I/R exposure.

B. Dot-density plots with median values and SD bars were used to represent the percent of immunoreactive areas of MBP (left) and GFAP (middle) as a ratio to the total microscopic field, and the ratio of the immunoreactive areas of MBP to GFAP (right). There were no differences in the ratio of the percentage of MBP immunoreactive area the to the total microscopic field area among the study groups (Kruska-Wallis, P=0.17). The cerebral cortex subjected to I/R (Isch-PL) demonstrated a reduction in immunohistochemically detectable GFAP compared with the Control (Kruska-Wallis, $P<0.03$) animals. Statistical differences were also not observed in the ratio of the GFAP immunoreactive areas to the total microscopic field between the Isch-mAb and the Control group (Kruska-Wallis, $P=0.54$) or between the Isch-PL and Isch-mAb groups (Kruska-Wallis, $P=0.46$). Differences were also

not observed in the ratio of immunoreactive area of MBP to GFAP (Kruska-Wallis, P>0.05) among Control, Isch-PL, and Isch-mAb groups.

Table 1

Pathological scores on ovine fetal gray and white matter, and parasagittal gray and white matter after exposure to ischemia with reperfusion injury for 24 h.

Groups	Brain Regions			
	Gray matter	White matter	Parasagittal gray matter	Parasagittal white matter
	Median (range)	Median (range)	Median (range)	Median (range)
Control (n=4–5)	0 (0–1)	0 (0–0)	0 (0–0)	0 (0–1)
Isch-PL (n=11)	1.5 * (0–5)	3 * (0–5)	1.5 * (0–5)	3 * (0–5)
Isch-mAb (11–12)	1.0 * (0–3.5)	1.0 * (0–4.5)	1.0 * (0–3.5)	1.0 * (0–4.5)

Values = median (range), Control = non-ischemic brain, Isch-PL = placebo-treated ischemic brain, Isch-mAb = anti-IL-1β-mAb-treated ischemic brain. SAS GLIMMIX generalized mixed modeling was used for statistics, and Least Squares Means was used for group differences.

*
P<0.05 vs control.